Analytical Methods

ROYAL SOCIETY OF CHEMISTRY

PAPER

View Article Online
View Journal | View Issue

Cite this: *Anal. Methods*, 2025, **17**, 7184

An innovative sampling device for size-fractionating airborne particulate matter for improved air pollution control of metal(oid)s and polycyclic aromatic hydrocarbons

Anja Ilenič, [ac] Radmila Milačič Ščančar, [bc] Marija Đurić, [a] Alenka Mauko Pranjić[a] and Janez Ščančar *[bc]

A sampling device was developed for collecting and size-fractionating airborne particulate matter (PM). A low-volume cascade system with polytetrafluoroethylene membrane filters (PM_{10}, $PM_{2.5}$, and $PM_{0.1}$) connected to an ultrapure-water trap was used to retain the $PM_{<0.1}$ fraction that passed through the filters. In the collected samples, metal(oid)s and platinum group elements (PGEs) were determined by inductively coupled plasma mass spectrometry after microwave-assisted digestion using a mixture of acids. Polycyclic aromatic hydrocarbons (PAHs) were extracted with a solvent mixture of acetone and petroleum ether, assisted by mechanical shaking and determined by gas chromatography mass spectrometry. The analytical methods were optimised and validated using the urban PM Standard Reference Material 1648a. Measurement repeatability and accuracy were 6% and 2% for metal(oid)s and PGEs, and 3% and 6% for PAHs, respectively. Field emission scanning electron microscopy analysis confirmed that the sampling device efficiently fractionated airborne PM to nano-sized particles. The sampling device was successfully applied to collect PM, enabling effective air pollution monitoring in urban areas. Analysis revealed that metal(oid)s were most abundant in PM_{10}, while those originating from traffic were also elevated in $PM_{<0.1}$. High-molecular-weight PAHs were distributed between PM_{10} and $PM_{2.5}$ fractions. The sampling device provides valuable insights into the chemical composition of (ultra) fine particles, overcoming the limitations of filter-based PM fractionation and providing improved air pollution control for nanoparticle-bound pollutants.

Received 19th May 2025
Accepted 7th August 2025

DOI: 10.1039/d5ay00858a

rsc.li/methods

Introduction

Urban air pollution is characterised by high levels of airborne particulate matter (PM), a heterogeneous mixture of natural (*e.g.* sea salt, dust, volcanic ash, pollen, fungal spores and forest fires) and anthropogenic (*e.g.* biomass burning, traffic, industry and construction activities) particles.[1–5] The behaviour and toxicity of PM in the atmosphere and within the human respiratory system are primarily influenced by particle size. Coarse particles (aerodynamic diameter >2.5 μm) tend to deposit in the nasopharynx, while fine particles (aerodynamic diameter <2.5 μm) and ultrafine particles (aerodynamic diameter <0.1 μm) can penetrate deep into the terminal bronchioles and alveoli.

Numerous epidemiological and toxicological studies have linked air pollution to adverse health effects and related health risks.[6–8] Even limited exposure can lead to oxidative stress at the air-lung interface, contributing to acute and chronic cardiopulmonary diseases, as well as neurodegenerative and reproductive disorders.[9–14] These effects are more pronounced with fine and ultrafine particles, as 50% of these particles remain in the lung parenchyma.[15] Additionally, fine and ultrafine particles have longer atmospheric residence times, ranging from a few hours to weeks, until they are removed by either wet or dry deposition.[16] Studies have shown that toxicity of PM per mass unit increases as particle size decreases, indicating that fine particles are more toxic than coarser ones.[17,18] This increased toxicity is primarily due to the larger total porous surface area of finer particles, which enables them to more easily adsorb and retain toxic substances.[15]

Understanding the relationship between chemical composition and sizes of particles is crucial, but published data indicate that this remains limited. Most research on airborne pollutants involves the use of high-volume samplers (>100 L min^{-1}) to collect larger sample quantities, enabling the detection of compounds with lower limits of detections (LODs).[19–22] However, increased air flow rates can potentially reduce the adsorption capacity of filters and increase the likelihood of filter clogging,

[a]*Department of Materials, Slovenian National Building and Civil Engineering Institute, Ljubljana, Slovenia. E-mail: janez.scancar@ijs.si*
[b]*Department of Environmental Sciences, Institute Jožef Stefan, Ljubljana, Slovenia*
[c]*Jožef Stefan International Postgraduate School, Ljubljana, Slovenia*

making them less suitable for accurately assessing human health risks during daily commuting. People typically inhale 10 to 15 times per minute, equating to about 6 L min^{-1}, making low-volume samplers (10 L min^{-1}) more suitable alternatives for human health risk assessments.[23–28]

Adequate sampling techniques are particularly important for detecting pollutants present at very low concentrations, such as metal(oid)s and polycyclic aromatic hydrocarbons (PAHs), which pose significant health and environmental risks. The United States Environmental Protection Agency (US EPA) has identified 16 priority PAHs for analysis in various environmental samples.[29] Among these, benzo[*a*]pyrene (BaP) is recognised as one of the most potent carcinogens. Other PAHs, such as benzo[*a*]anthracene (BaA), benzo[*b*]fluoranthene (BbF), benzo[k]fluoranthene (BkF), chrysene (Ch) and indeno[1,2,3-*cd*]pyrene (IP) are classified as possibly carcinogenic to humans.[30,31] Among metal(oid)s, arsenic (As), hexavalent chromium (Cr(VI)), cadmium (Cd), nickel (Ni), and lead (Pb) are of particular concern as carcinogenic airborne contaminants.[32] Accurate chemical analysis of these PAH compounds and metal(oid)s is essential across all inhalable PM sizes, including nanoparticles, which are often overlooked.

Previous studies have reported PAHs in size-fractioned PM_{10} and $PM_{2.5}$ (ref. 33–35) and metals in size-fractioned PM_{10} and $PM_{2.5}$.[36–38] However, the simultaneous determination of both types of pollutants in different PM sizes is rarely reported.[39,40] Very few studies performed characterisation of PM of smaller fractions.[41–44] Physio-chemical analyses of samples collected on filters by low-volume cascade samplers present significant challenges, mainly due to the small amount of the PM collected. Therefore, highly sensitive analytical techniques such as inductively coupled plasma mass spectrometry (ICP-MS) and gas chromatography mass spectrometry (GC-MS) are used for chemical analysis of samples. Analytical methods with high selectivity, resolution and sensitivity must be applied to provide data for reliable assessment of health and environmental hazards. However, only a few atmospheric studies report the use of certified reference materials (CRMs). These materials are analysed to check the accuracy of results and validate the analytical procedures.[26,45–47]

Given that pollutants bound to airborne (ultra)fine particles have the most harmful effects on human health, it is essential to improve pollution control measures and enhance risk assessment strategies by taking into account various PM fractions, including the nano-sized PM particles. Therefore, the objectives of our work were (i) to develop a low-volume cascade sampling device for collecting and size-fractionating airborne PM, consisting of polytetrafluoroethylene (PTFE) membrane filters (PM_{10}, $PM_{2.5}$, and $PM_{0.1}$) connected to an ultrapure-water trap designed to retain the $PM_{<0.1}$ fraction; (ii) to verify the size of PM particles collected on filters using field emission scanning electron microscopy (SEM) analysis; (iii) to optimise and validate analytical methods for the determination of metal(oid)s, including platinum group elements (PGEs) using ICP-MS, and PAHs in the collected sample fractions using GC-MS; and (iv) to analyse the concentrations of metal(oid)s and PAHs in collected samples at different urban locations in Slovenia using the developed sampling device, placed within one metre of bicycle lanes, in order to assess the air pollution-related health risks for daily commuters.

Experimental

Instrumentation

Total elemental concentrations were determined by ICP-MS on an Agilent 7900 instrument (Agilent Technologies, Tokyo, Japan). The ICP-MS operating parameters are presented in Table S1 (SI). Data were acquired using Agilent MassHunter 5.1 software and further processed with Microsoft Excel 2019 (Redmond, WA, USA).

PAH determination was carried out by GC-MS, using an Agilent HP6890 GC (Agilent Technologies, Tokyo, Japan) with a 5973 mass selective detector (MSD) and equipped with an Agilent 6890 Series autosampler injector. PAHs were separated on an Agilent capillary column HP-5MS (30 m × 0.25 mm, film thickness 0.25 μm) coated with 5% phenylmethylpolysiloxane. The GC-MS operating parameters are presented in Table S2.

A Milestone ETHOS UP Microwave Digestion System (Sorisole, Italy) was used for sample digestion in the analysis of metal(oid)s and PGEs. For PAH analysis, the samples were mechanically shaken using a Vibromix 40 orbital shaker (Tehtnica, Železniki, Slovenia). The sample extracts were concentrated using a sample concentrator Dri-Block Heater DB100/3 (Techne Inc., Vernon Hills, IL, USA). A Mettler AE 163 analytical balance (Zürich, Switzerland) was used for weighing.

Morphological analysis of airborne PM was conducted using SEM with a Zeiss ULTRA plus scanning electron microscope (Carl Zeiss AG, Oberkochen, Germany) equipped with an energy dispersive X-ray spectrometer (EDS) system manufactured by Oxford Instruments (High Wycombe, UK).

A Vacuubrand (Wertheim, Germany) low-volume diaphragm pump ME 1C (100 mbar, 0.8 m^3 h^{-1}) was used for sampling of real airborne PM, while air flow through the system was measured using a G1.6 gas meter (Dadolab, Cinisello Balsamo, Italy). The air flow rate was controlled using a variable area flow meter DK46/800 (Krohne, Wellingborough, UK). PM was collected using a three-stage cascade NILU polycarbonate filter holder system (Innovation NILU, Kjeller, Norway) equipped with hydrophobic Whatman PTFE membrane filters (pore sizes of 10 μm, 2.5 μm and 0.1 μm and diameters of 47 mm) obtained from Merck (Darmstadt, Germany).

Reagents and materials

An ultrapure water system (PURELAB Flex 3, ELGA, LabWater, UK) was used for the preparation of samples and reagents.

For metal(oid)s analysis, Suprapur nitric acid (67–70% HNO_3) was obtained from Carlo Erba Reagents (Val-de-Reuil, Normandie, France), while Suprapur hydrochloric acid (30% HCl) and Suprapur hydrofluoric acid (40% HF) were purchased from Merck (Darmstadt, Germany). ICP multi-element standard solution XVI (21 elements in diluted nitric acid, 100 mg L^{-1}, part no. 1.09487.0100) was used to prepare calibration curves for the metal(oid)s arsenic (As), cadmium (Cd), chromium (Cr), cobalt (Co), copper (Cu), molybdenum (Mo), nickel (Ni), lead

(Pb), thallium (Tl), vanadium(v) and zinc (Zn). For barium (Ba), a single standard (1000 ± 2 mg L^{-1} in 2–3% HNO_3, part No. 1.70304.0100) was used. Single standard solutions of palladium (Pd) (1000 ± 2 mg L^{-1} in 0.5 mol L^{-1} HNO_3, part no. 1.14282.0100) and platinum (Pt) (1000 ± 2 mg L^{-1} in 2 mol L^{-1} HCl, part no. 1.102645.0100) were used to prepare the calibration curve for PGEs. Stock standard solutions of germanium (Ge), rhodium (Rh) (1000 ± 2 mg L^{-1} in 2–3% HNO_3, part Nos. 1.70320.0100 and 1.02650.0100, respectively), and iridium (Ir) (1000 ± 2 mg L^{-1} in 7% HCl, part no. 1.70325.0100) were used to prepare internal standards in ICP-MS analysis. All standard solutions were purchased from Merck.

For PAH analysis, acetone (C_3H_6O) and petroleum ether, both purchased from Merck, were used for extraction of the high-molecular weight PAHs benzo[*a*]anthracene (BaA), benzo[*a*]pyrene (BaP), benzo[*b*]fluoranthene (BbF), benzo[ghi]perylene (BghiP), chrysene (Ch), fluoranthene (Fl), indeno[1,2,3-*cd*]pyrene (IP) and pyrene (P). Anhydrous sodium sulphate (Na_2SO_4) from Merck was used for water removal from the organic phase. Strata FL-PR Florisil (activated magnesium silicate, MgO_3Si, 170 μm, 80 Å, 500 mg^3 mL^{-1}; Phenomenex, Inc., Torrance, CA, USA) was used for the cleaning of sample extracts. A standard stock solution PAH-Mix 9 (10 μg mL^{-1}, part no. DRE-XA20950009CY) in cyclohexane, containing 16 analytes, was used to create calibration curves for the determination of PAHs by GC-MS. A deuterated PAH-Mix 9 (10 μg mL^{-1}, part no. DRE-L20950902CY) in cyclohexane, also containing 16 analytes, was used as an internal standard. Both the PAH-Mix standard and internal standard were purchased from LGC (Teddington, UK). Isooctane (2,2,4-trimethylpentane) obtained from Merck was used as a reference standard to calibrate the GC-MS system. The retention times of PAHs in the samples were compared to the retention time of isooctane, aiding in the identification of PAHs during the GC-MS analysis. A typical chromatogram illustrating the separation of the PAH-Mix 9 standard solution (16 PAHs, 500 ng mL^{-1}) and the deuterated PAH-Mix 9 (16 PAHs-D, 500 ng mL^{-1}) used as an internal standard, applying the GC-MS procedure, with PAHs considered for analysis marked in red, is presented in Fig. S1. Retention times of the separated PAHs and deuterated PAH compounds are presented in Table S3. The certified standard reference material SPS-SW1 (reference material for measuring elements in surface waters), obtained from Spectrapure Standards (Oslo, Norway), was used daily during ICP-MS analysis to verify the accuracy of the calibration curves and measurement procedures for metal(oid)s. Standard Reference Material (SRM) 1648a (Urban Particulate Matter) from the National Institute of Standards and Technology (NIST) (Gaithersburg, MD, USA), certified for selected elements and PAHs, was employed to verify the accuracy of metal(oid) determinations in digested PM, as well as PAHs in the extracted PM from both the filters and the aqueous phase. This SRM was also used to optimise and validate the analytical procedures.

Sampling sites and sample collection

Sampling of airborne PM was carried out from December 1, 2023, to December 31, 2023, at three different urban settings in Slovenia: Dobrova (DB: 46.067450, 14.409407), Ljubljana (LJ: 46.033985, 14.518328) and Maribor (MB: 46.548294, 15.649047). Sampling points were positioned at the ground level at an average human height (170 cm), within one metre of bicycle lanes. Samples were collected monthly using an innovative sampling device, consisting of two identical units – one for metal(oid)s and the other for PAHs. The units were installed in a metal cage to protect them from damage caused by precipitation and vandalism, while ensuring uninterrupted access to the surrounding air (Fig. S2).

The sampling unit consisted of a three-stage cascade filter holding system incorporating hydrophobic PTFE membrane filters with pore sizes of 10 μm, 2.5 μm and 0.1 μm (Fig. S3). This cascade filter system was connected to the water trap inside a 2000 mL amber glass Pyrex burette bottle in order to retain the nano-sized particles ($PM_{<0.1}$). The air volume passing through the system was controlled by using a low-volume diaphragm pump connected to a gas meter. Prior to the sample analysis, the stability of the airflow rate of a low-volume diaphragm pump was monitored continuously over one month using a flow meter.

After the sampling, the nano-sized $PM_{<0.1}$ fraction (captured in a water trap) and the PTFE membrane filters were stored at −15 °C until analysis. Each filter and the aqueous phase of the nano-sized $PM_{<0.1}$ fraction represented the total monthly amount of PM. The volume of air pumped through the sampling unit was monitored throughout the entire sampling period, allowing for the reporting of metal(oid) and PAH concentrations in ng m^{-3} of air.

Optimized analytical procedures for the analysis of metal(oid)s and PGEs by ICP-MS

To avoid contamination, all glassware was soaked in 10% HNO_3 for 48 h, rinsed three times with ultra-pure water and dried at 80 °C. Teflon vessels were cleaned with 10% HNO_3 using the same protocol as that for the microwave-assisted digestion of samples. The vessels were then rinsed three times with ultra-pure water and kept at 150 °C for 6 h, in order to remove any residual HNO_3 vapours.

After sampling, filters (PM_{10}, $PM_{2.5}$, and $PM_{0.1}$) were weighed, cut in half with iron scissors, and aliquots of the filters were weighed again to accurately determine the proportion of the whole PM collected in each aliquot. The nano-sized $PM_{<0.1}$ collected in the 1 L water trap was acidified with 1 mL of HNO_3, evaporated to 20 mL in a sand bath at 200 °C, and then divided into two 10 mL aliquots. One half of the filters (PM_{10}, $PM_{2.5}$, and $PM_{0.1}$) and one aliquot of the nano-sized $PM_{<0.1}$ fraction were used for the analysis of metal(oid)s, while the other half was used for the analysis of PGEs.

For the determination of metal(oid)s, 3 mL of HNO_3, 1 mL of HCl and 0.2 mL of HF were used in microwave-assisted digestion, while for the determination of PGEs, *aqua regia* (3 mL of HCl and 1 mL of HNO_3) with the addition of 0.2 mL of HF was used. Samples were subjected to closed-vessel microwave-assisted digestion, using the following temperature programme: ramp to 140 °C for 15 min, hold at 140 °C for 5 min,

ramp to 200 °C for 20 min, hold at 200 °C for 60 min, and cool down for 30 min. The clear digests of the filters and the nano-sized $PM_{<0.1}$ aqueous phase fraction were quantitatively transferred to 30 mL polypropylene graduated tubes and filled to the mark with ultra-pure water. Concentrations of metal(oid)s in digested samples were determined by ICP-MS using external calibration for quantification. The same analytical procedures, with no samples added, were applied to determine procedural blanks. Concentrations of metal(oid)s and PGEs in the procedural blanks were below the LODs, or did not exceed 3% of the measured elemental concentrations.

Optimized analytical procedures for the analysis of PAHs by GC-MS

To avoid contamination, all glassware was rinsed three times with tap water, soaked in 10% nitric acid for 48 h, rinsed three times with tap water and three times with ultra-pure water and heated at 400 °C for at least 4 h. Prior to use, all glassware was rinsed with petroleum ether and acetone and dried at room temperature.

After sampling, PAHs collected on the filters (PM_{10}, $PM_{2.5}$, and $PM_{0.1}$) and the nano-sized $PM_{<0.1}$ fraction retained in the aqueous phase were extracted using organic solvents. The filters were transferred to Erlenmeyer flasks, and a mixture of 15 mL of acetone and petroleum ether (1 : 1, *v*/*v*) and 100 μL of isooctane was added. The samples were then spiked with 50 μL of an internal standard solution (10 μg mL^{-1}) and shaken on a mechanical shaker for 16 h at 180 rpm.

For the nano-sized $PM_{<0.1}$ fraction, a liquid–liquid extraction (LLE) was performed. A mixture of 100 mL of acetone and petroleum ether (1 : 1, *v*/*v*) along with 100 μL of isooctane was added to 1 L of the sample. After spiking with 50 μL of the internal standard solution (10 μg mL^{-1}), the mixture was shaken for 16 h at 180 rpm. The content was quantitatively transferred into a glass separatory funnel to separate the organic phase from the aqueous phase. Traces of water in the organic phase were removed using anhydrous Na_2SO_4, and pre-heated at 550 °C for 6 h.

The organic phase from both the filter extracts and the nano-sized $PM_{<0.1}$ fraction was passed through a 3 mL column filled with Florisil for sample clean-up. The organic phase was concentrated to approximately 1 mL under a nitrogen stream at 40 °C using a sample concentrator. The concentrated samples were then transferred to 2 mL amber vials with a Pasteur pipette and sealed. Finally, 1 μL of the sample was injected onto the column for the determination of PAHs by GC-MS, using external calibration for quantification. The same analytical procedure, with no samples added, was applied to determine procedural blanks. Concentrations of PAHs in the procedural blanks were below the LODs.

A flow chart illustrating the optimised analytical procedures for the determination of metal(oid)s, PGEs and PAHs is presented in Fig. 1.

Morphological analysis

SEM-EDS was used to examine particle sizes and shapes (morphology), the chemical composition of selected elements in PM and the size distribution of particles collected on filters. The analysis was conducted in high-vacuum mode (pressure of 25 Pa) with an accelerating voltage of 8–10 kV. For SEM analysis, PM was collected on PTFE filters (with pore sizes of 10 μm, 2.5 μm and 0.1 μm) over two days, after the experiments for the analysis of metal(oid)s and PAHs. In prior microstructural analysis, samples were coated with a 15 nm layer of carbon or gold to enhance conductivity and mitigate electron charging. A

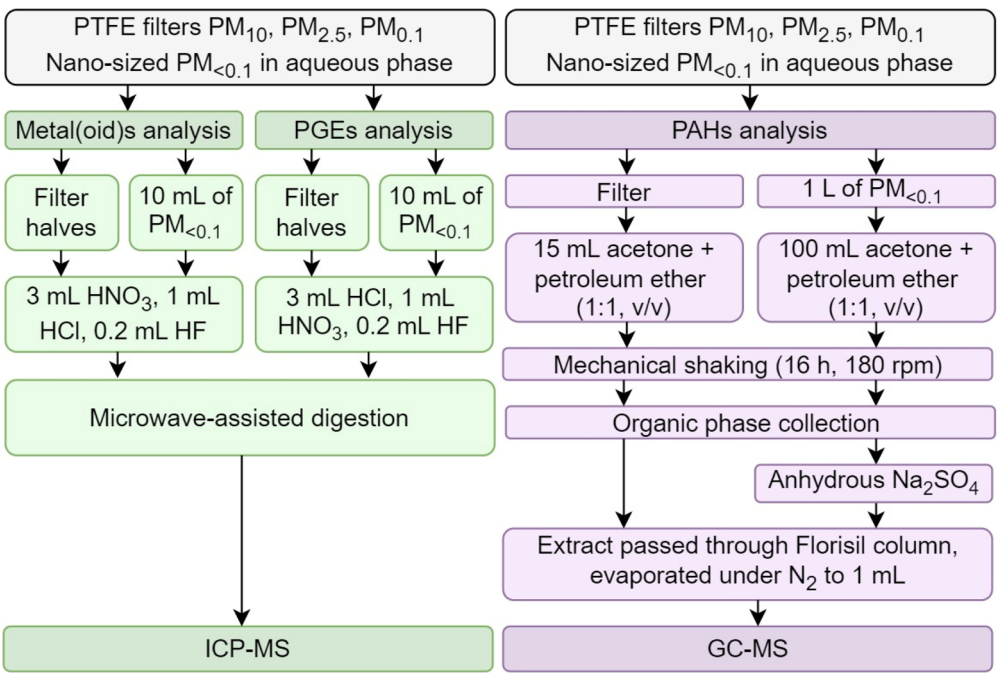

Fig. 1 Flow chart of the optimised analytical procedures for the determination of metal(oid)s, PGEs and PAHs in size-fractionated airborne PM.

gold coating was chosen as it resulted in lower electron charging and enabled the use of higher magnifications.

Optimization of the analytical procedures

The analytical procedures for the determination of metal(oid)s, PGEs and PAHs were optimised using urban dust SRM 1648a. This SRM was chosen due to its similarity to the sample matrix and its certified values for both analytes – metal(oid)s and PAHs. Aliquots of approximately 40 mg were used for the analysis, as the homogeneity of SRM was confirmed for sample amounts larger than 5 mg in the NIST Certificate of Analysis.[48] For the optimisation of analytical procedures, experiments were carried out in duplicate. The performance of the optimised analytical procedures for the analysis of metal(oid)s, PGEs and PAHs was evaluated by determining the repeatability of measurements, the limits of detection (LODs), limits of quantification (LOQs), and linearity and by performing an accuracy check.

Analytical procedures for the determination of metal(oid)s and PGEs by ICP-MS

To achieve effective decomposition of the sample matrix for metal(oid)s or PGEs, 3 mL of HNO_3 and 1 mL of HCl (for nitric acid digestion) or 3 mL of HCl and 1 mL of HNO_3 (for *aqua regia* digestion) were added to the urban dust SRM, along with varying amounts of HF, using microwave-assisted digestion. The ICP-MS analysis revealed that the addition of HF was crucial for the dissolution of silicates, which can occlude metal(loid)s and PGEs in the PM. The optimal amount of HF added was 0.2 mL. The procedure optimised for the urban dust SRM sample was subsequently applied to the determination of metal(oid)s and PGEs in PM_{10}, $PM_{2.5}$ and $PM_{0.1}$ fractions collected on filters, as well as the $PM_{<0.1}$ fraction retained in the aqueous phase, as described in the section Optimised analytical procedures for the analysis of metal(oid)s and PGEs.

The studied metal(oid)s and PGEs were selected due to their association with traffic emissions from the wear of engine parts, lubricants and additives used in gasoline (Ba, Cr, Cu, Mo, Pb, V, and Zn),[38,49] and emissions from diesel fuels (Ba, Cd, Cr, Mo, Ni, V, and Zn),[49,50] brake pads (Ba, Cu, and Mo) and tyre wear (Ba, Cd, and Zn),[38] as well as their use as catalysts to control car exhaust emissions (Pd and Pt).[51]

Figures of merit for the determination of metal(oid)s and PGEs in urban dust

The repeatability of metal(oid) measurements was tested by performing six analyses of SRM 1648a using nitric acid digestion, while the repeatability of measurement of PGEs was checked by analysing six SRM 1648a samples with *aqua regia* digestion. The results for repeatability, calculated as the relative standard deviation (RSD), are presented in Table 1.

Good repeatability of measurement was obtained for metal(oid)s, with an average of RSD 6% and accuracy of 2%. However, the repeatability for Pt and Pd was lower, with RSDs of 21% and 17%, respectively, due to their low concentrations in the urban dust samples analysed.

The LODs and LOQs for the determination of individual metal(oid) and PGE concentrations in the sample digests were calculated as the concentration that provided signals equal to 3s or 10s of the blank sample, respectively. To calculate the LODs and LOQs, 8 blank samples (acids used for digestion) were analysed by ICP-MS. The LODs and LOQs for metal(oid)s and PGEs, expressed in ng mL^{-1}, and for urban dust samples expressed in mg kg^{-1}, are provided in Table S4. Values expressed in ng m^{-3} are presented in Table S5. Low LODs, ranging from 0.001 to 0.02 ng mL^{-1} were achieved, enabling the quantification of metal(oid)s and PGEs in urban dust and airborne PM using the optimised analytical procedures.

The linearity of measurement for metal(oid)s and PGEs ranged from the LOQ to 1000 ng mL^{-1}, with correlation coefficients (R^2) for the calibration curves better than 0.998.

The accuracy of the optimised analytical procedures was verified by analysing SRM 1648a and comparing the determined concentrations with the certified concentrations. For elements

Table 1 Concentrations of metal(oid)s in SRM 1648a (urban particulate matter) determined after nitric acid microwave-assisted digestion and PGEs after *aqua regia* microwave-assisted digestion by ICP-MS. The results represent the concentrations of six individual samples, along with RSDs between the parallel samples

Element	Concentration (mg kg^{-1})	Concentration (mg kg^{-1})	Concentration (mg kg^{-1})	Concentration (mg kg^{-1})	Concentration (mg kg^{-1})	Concentration (mg kg^{-1})	Average (mg kg^{-1})	RSD (%)
As	127	129	123	120	118	109	119	5.4
Ba	801	812	807	806	805	815	808	0.6
Cd	75.0	72.8	74.5	71.3	73.4	73.6	73.4	1.6
Co	18.7	19.1	18.6	18.4	17.3	19.0	18.5	3.3
Cr	390	400	391	367	384	426	393	4.5
Cu	738	748	748	749	700	658	724	4.7
Mo	22.6	21.1	22.9	21.4	22.9	21.3	22.0	3.5
Ni	85.3	86.4	87.5	85.7	82.3	76.5	84.0	4.4
Pb	6527	6374	6455	6544	6359	6441	6450	1.1
Pd	0.69	0.49	0.52	0.62	0.50	0.41	0.54	17
Pt	0.041	0.027	0.040	0.022	0.030	0.033	0–032	21
Tl	1.87	1.91	1.96	1.81	1.86	1.66	1.85	5.6
V	137	139	153	150	140	131	142	5.3
Zn	5241	5260	4744	4561	4610	4263	4780	7.6

Table 2 Concentrations of metal(oid)s in SRM 1648a (urban particulate matter) determined after nitric acid microwave-assisted digestion and PGEs after *aqua regia* microwave-assisted digestion by ICP-MS. The results from a spike recovery test are provided for elements that are not certified. The results represent the mean concentration obtained from six parallel samples ± standard deviation between the parallel samples

Element	Determined concentration (mg kg^{-1})	Certified concentration (mg kg^{-1})	Added concentration (mg kg^{-1})	Found concentration (mg kg^{-1})	Relative recovery (%)
As	121 ± 2.9	115.5 ± 3.9	—	—	—
Ba	808 ± 2.0	—	472	1321	103
Cd	73.4 ± 0.5	73.7 ± 2.3	—	—	—
Co	18.5 ± 0.3	17.93 ± 0.68	—	—	—
Cr	393 ± 7.9	402 ± 13	—	—	—
Cu	724 ± 15.2	610 ± 70	—	—	—
Mo	22.0 ± 0.3	—	18.9	41.3	101
Ni	84.0 ± 1.6	81.1 ± 6.8	—	—	—
Pb	6450 ± 31.1	6550 ± 330	—	—	—
Pd	0.54 ± 0.04	—	9.5	10.24	98.5
Pt	0.032 ± 0.003	—	14.35	13.83	96.2
Tl	1.85 ± 0.04	—	1.9	3.6	97.3
V	142 ± 3.3	127 ± 11	—	—	—
Zn	4780 ± 162	4800 ± 270	—	—	—

not certified in SRM 1648a, a spike recovery test was applied. The sample was spiked with an appropriate amount of selected elements before microwave-assisted digestion. Nitric acid digestion was used for Ba, Mo and Tl, and *aqua regia* digestion for Pd and Pt. The relative recovery, expressed as a percentage, was calculated as the ratio between the found and expected concentrations (the sum of the element concentration in urban dust and the added concentration) multiplied by 100. The results are presented in Table 2.

It is evident that the determined concentrations are in good agreement with the certified values. The relative recoveries of the spiked elements ranged between 96% and 103%, indicating quantitative determination of Ba, Mo, Pd, Pt and Tl in urban dust samples. Therefore, it can be concluded that the optimised analytical procedures provide accurate results for the analysis of the studied metal(oid)s and PGEs.

Analytical procedures for the determination of PAHs by GC-MS

The procedure was modified based on the extraction methods described in SIST ISO 18287:2019; SIST EN 15549:2008; and SIST EN 15527:2009,[52–54] using acetone and petroleum ether. This modification involved reducing the amount of extracting agent and optimizing the extraction duration and the clean-up step. PAHs in the petroleum ether extract were quantified according to the method described in ISO 28540:2011[55] for PAH determination in water samples by GC-MS.

Initially, extraction was performed using a 100 mL mixture of acetone and petroleum ether (1 : 1, *v*/*v*). However, due to the small quantity of the sample, it was experimentally found that the volume of the extracting agent can be significantly reduced. For a 40 mg urban dust SRM sample, a mixture of 15 mL of acetone and petroleum ether (1 : 1, *v*/*v*), along with 100 μL of isooctane, was added. The samples were spiked with 50 μL of an internal standard solution (10 μg mL^{-1}) and subjected to microwave-assisted extraction (40 °C, 600 W) for 1 h, or shaken on a mechanical shaker for 16 h or 24 h (25 °C, 180 rpm).

The organic phase was passed through a 3 mL column filled with Florisil for sample clean-up and concentrated to approximately 1 mL under a nitrogen stream at 40 °C using a sample concentrator. GC-MS analysis indicated that samples shaken for 16 h achieved better recovery rates than those shaken for 24 h (recoveries greater than 7% and 11%, respectively), while the recovery rate for microwave-assisted extraction was lower (14%). Thus, mechanical shaking for a duration of 16 h was chosen as the optimal extraction procedure, followed by the clean-up step. Additionally, the results indicated that a single cleaning of the organic phase with Florisil yielded better recoveries compared to a double cleaning (recoveries of 7% and 11%, respectively). Consequently, a single cleaning procedure was employed for the petroleum ether extract containing SRM urban dust.

The optimised procedure was then applied to the determination of PAHs in the PM_{10}, $PM_{2.5}$ and $PM_{0.1}$ fractions collected on filters and for the $PM_{<0.1}$ fraction retained in the aqueous phase, as described in the section Optimised analytical procedure for the analysis of PAHs.

In this study, PAHs were investigated due to their common presence as organic contaminants in urban dust and PM, originating from vehicle exhaust, combustion processes and industrial activities.[56,57] The following 8 PAHs were selected for monitoring due to their high toxicity and prevalence in the environment: BaA, BaP, BbF, BghiP, Ch, Fl, IP, and P.[31]

Figures of merit for the determination of PAHs in urban dust

The repeatability of measurement of PAHs was evaluated by performing six analyses of SRM 1648a. The repeatability results, calculated as the RSD, are presented in Table 3.

The results in Table 3 demonstrate good repeatability of measurement, with an average RSD of 3% and accuracy of 6%.

The LODs and LOQs for the determination of concentrations of PAHs in sample extracts were calculated as the concentration that provided a signal equal to 3s or 10s of the blank sample, respectively. To calculate the LODs and LOQs, 8 blank samples (petroleum ether extract) were analysed by GC-MS. The LODs

Table 3 Concentrations of PAHs in SRM 1648a (urban particulate matter) determined after extraction into petroleum ether by GC-MS. The results represent the concentrations of six individual samples ± the standard deviation of measurement, along with RSDs between the parallel samples

PAH	Concentration (mg kg^{-1})	Concentration (mg kg^{-1})	Concentration (mg kg^{-1})	Concentration (mg kg^{-1})	Concentration (mg kg^{-1})	Concentration (mg kg^{-1})	Average (mg kg^{-1})	RSD (%)
BaA	2.63	2.56	2.52	2.56	2.59	2.59	2.58	1.3
BaP	2.39	2.27	2.30	2.20	2.37	2.32	2.31	2.8
BbF	7.70	8.88	8.48	8.33	7.90	8.04	8.22	4.8
BghiP	4.32	4.03	4.23	4.18	4.17	4.14	4.18	2.1
Ch	6.75	6.70	6.81	6.66	6.85	6.81	6.76	1.0
Fl	7.59	7.65	7.57	7.40	7.52	7.96	7.62	2.3
IP	4.08	4.55	4.15	4.16	3.95	3.78	4.11	5.7
P	6.03	6.00	5.92	5.86	5.98	6.16	5.99	1.6

and LOQs for PAHs, expressed in ng mL^{-1}, and for urban dust samples expressed in mg kg^{-1}, are provided in Table S6, and expressed in ng m^{-3} in Table S7. The LODs for the PAHs measured (4.5 ng mL^{-1}) were adequate for the quantification of PAHs in urban dust and airborne PM using the optimised analytical procedures.

The linearity of measurement for PAHs ranged from the LOQ to 1000 ng mL^{-1}, with correlation coefficients (R^2) for the calibration curves better than 0.997.

The accuracy of the optimised analytical procedures was verified by analysing SRM 1648a and comparing the determined concentrations with the certified values. The results are presented in Table 4.

Data from Table 4 show good agreement between the determined PAH concentrations. Deviations from the certified value did not exceed 10%, and the exception was only BghiP, for which the determined concentration was 16% lower than the certified value. These data confirm that the optimised analytical procedure provides accurate results for the analysis of the studied PAHs.

Flow rates of low-volume pumps during sampling of size-fractionating airborne particulate matter over 28 days

To check the variation in flow rates during the one-month air sampling period, 6 cascade sampling devices with PTFE membrane filters (PM_{10}, $PM_{2.5}$, and $PM_{0.1}$) and an ultrapure-water trap for retaining the $PM_{<0.1}$ fraction were connected to 6 low-volume pumps and placed outside. The flow rate of each pump was measured on days 0, 14, 21 and 28. The data on the measured flow rates are presented in Table S8. As shown, the flow rates for all 6 pumps remained relatively unchanged throughout the course of the experiment (12 L min^{-1}). This preliminary experiment confirmed that the low-volume cascade system enables continuous sampling over a one-month period without causing filter clogging.

Table 4 Concentrations of PAHs in SRM 1648a (urban particulate matter) determined after extraction into petroleum ether by GC-MS. The results represent the mean concentrations obtained from six parallel samples ± standard deviation between the parallel samples

PAH	Determined concentration (mg kg^{-1})	Certified concentration (mg kg^{-1})
BaA	2.58 ± 0.02	2.71 ± 0.15
BaP	2.31 ± 0.03	2.57 ± 0.10
BbF	8.22 ± 0.18	8.89 ± 0.05
BghiP	4.18 ± 0.04	5.00 ± 0.18
Ch	6.76 ± 0.03	6.12 ± 0.06
Fl	7.62 ± 0.08	8.07 ± 0.14
IP	4.11 ± 0.11	4.17 ± 0.17
P	5.99 ± 0.04	5.88 ± 0.07

Evaluation of morphological characteristics and particle size distribution of particulate matter collected on filters

Airborne particles are generally classified into geogenic, anthropogenic and biogenic categories. Geogenic particles, which originate naturally, include quartz, aluminosilicates, calcium-rich particles, chlorides and Fe/Ti oxides. Anthropogenic particles, predominantly carbonaceous and sulphates, are commonly associated with vehicular emissions and biomass burning.[58,59] Biogenic particles are typically characterised as pollen, fungal spores and plant debris, contributing significant portions to airborne PM.[60] The main aim was to determine the morphology and size of fractioned PM on filters using SEM-EDS (Fig. 2), to distinguish its potential sources.

The identified particles were classified into six morphological clusters (Fig. 2): spherules (P1, P7, P12, and P13), floccules (P2), biogenic particles (P3), tabular particles (P5 and P10), irregular shaped grains (P6 and P8) and agglomerate particles (P9 and P11). Most of the identified particles were non-spherical, thereby providing a higher surface area for potential toxic compound adsorption and enhancement of their interaction with lung tissues.[61] The most common particles found in this study include alumosilicates (P1), magnesium silicates (P7), and carbonate particles (P6), along with sulphates (P8 and P10) and carbon-enriched particles (P5) (Table S9).

Anthropogenic particles include spherules, floccules and agglomerates. Spherules are typically smaller, with an average diameter of less than 3 μm,[62–65] and generally exhibit a Si–Al–Fe elemental composition. Floccules consist of small spherical particles (<1 μm) with a loose structure, while agglomerates are characterised by flexuous, fractal edge branches or crinkles randomly distributed on the surface, forming a lump-like morphology. Agglomerate and spherical particles are typically

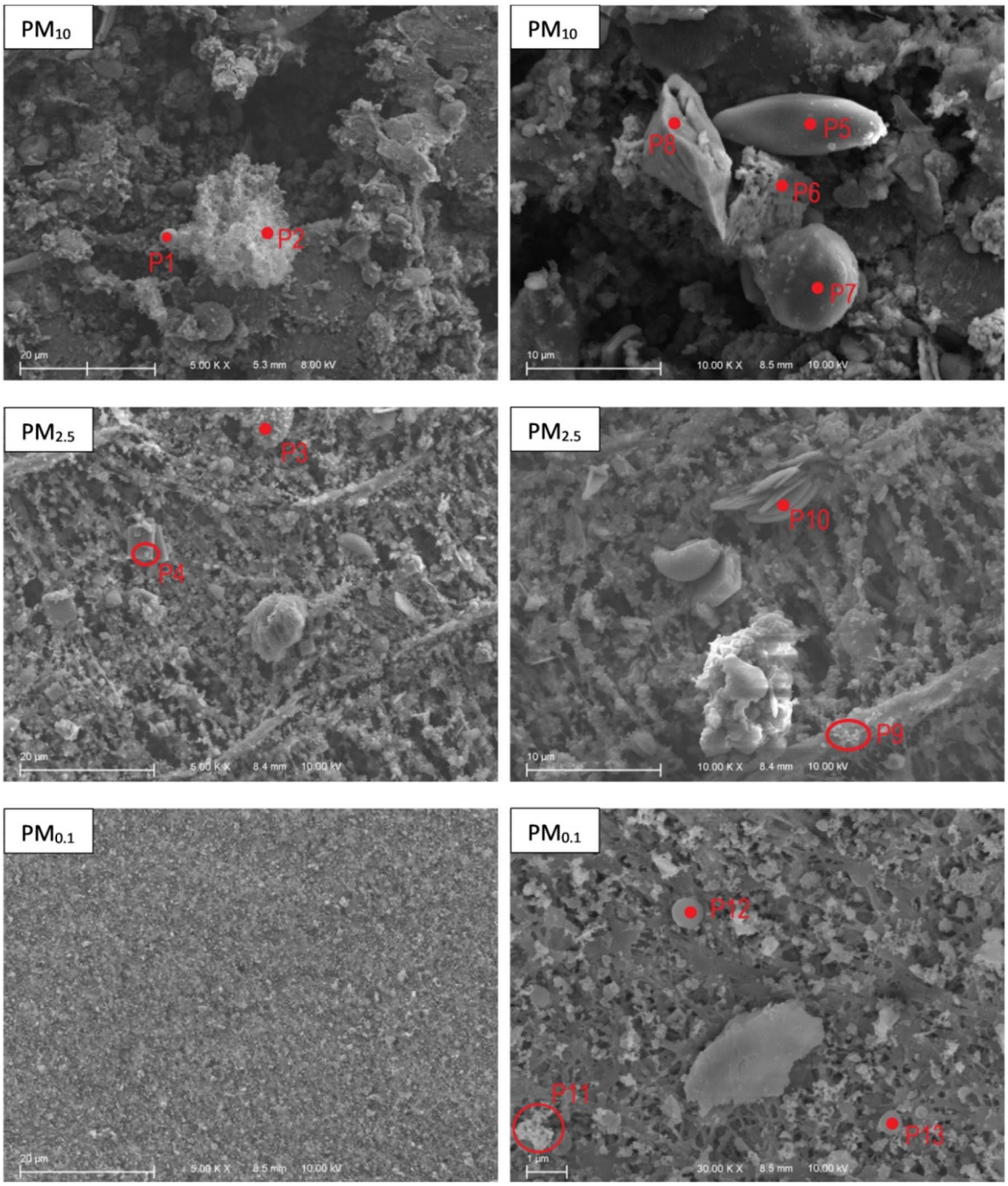

Fig. 2 SEM imaging of PM_{10} (left at 5000× magnification;right at 10 000× magnification), $PM_{2.5}$ (left at 5000× magnification; right at 10 000× magnification) and $PM_{0.1}$ (left at 5000× magnification; right at 30 000× magnification).

derived from coal combustion, while floccules result from vehicle emissions.[65]

Geogenic particles are mostly characterised by irregularly shaped grains, which exhibit smooth, flat surfaces (P5 and P8) or semi-coarse to coarse, holed surfaces (P6), with an average diameter of around 10 µm. These particles result from mechanical abrasion and originate from soil and surface deposits.[65] Tabular particles appear more elongated, either rectangular or elliptical, and are generally emitted through geogenic processes and biological activity.[65]

The SEM-EDS images show that the particles collected on filters align with the pore sizes of the filters used, confirming the reliability of the low-volume cascade PTFE membrane filter system for fractionating PM_{10}, $PM_{2.5}$ and $PM_{0.1}$ particle size fractions.

Analysis of metal(oid)s, PGEs and PAHs in size-fractionated particulate matter in urban settings in Slovenia

To demonstrate the applicability of the developed sampling device, size-fractionated PM was collected during December

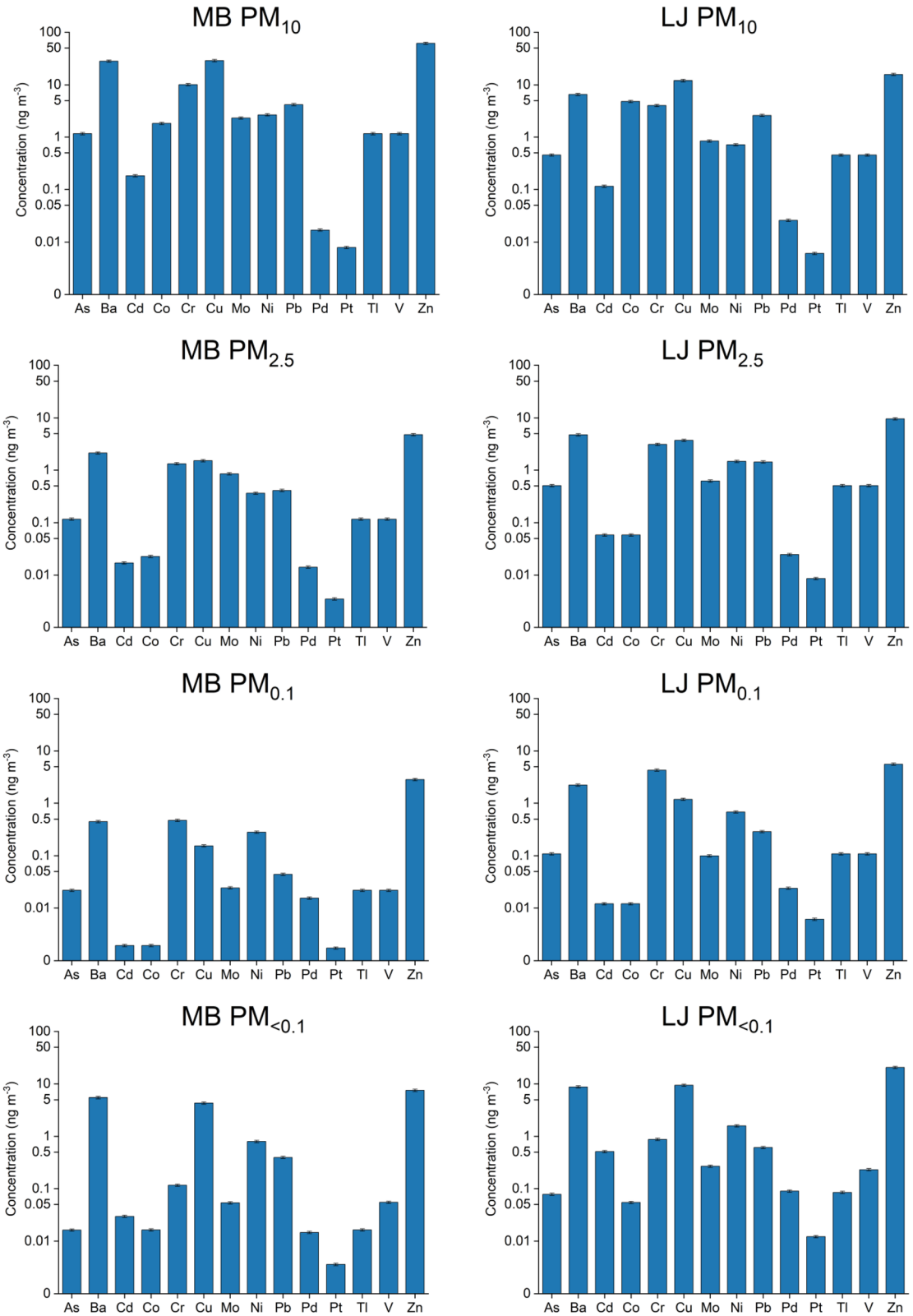

Fig. 3 The distribution of metal(oid)s in size-fractionated airborne PM in Maribor (MB), Ljubljana (LJ) and Dobrova (DB).

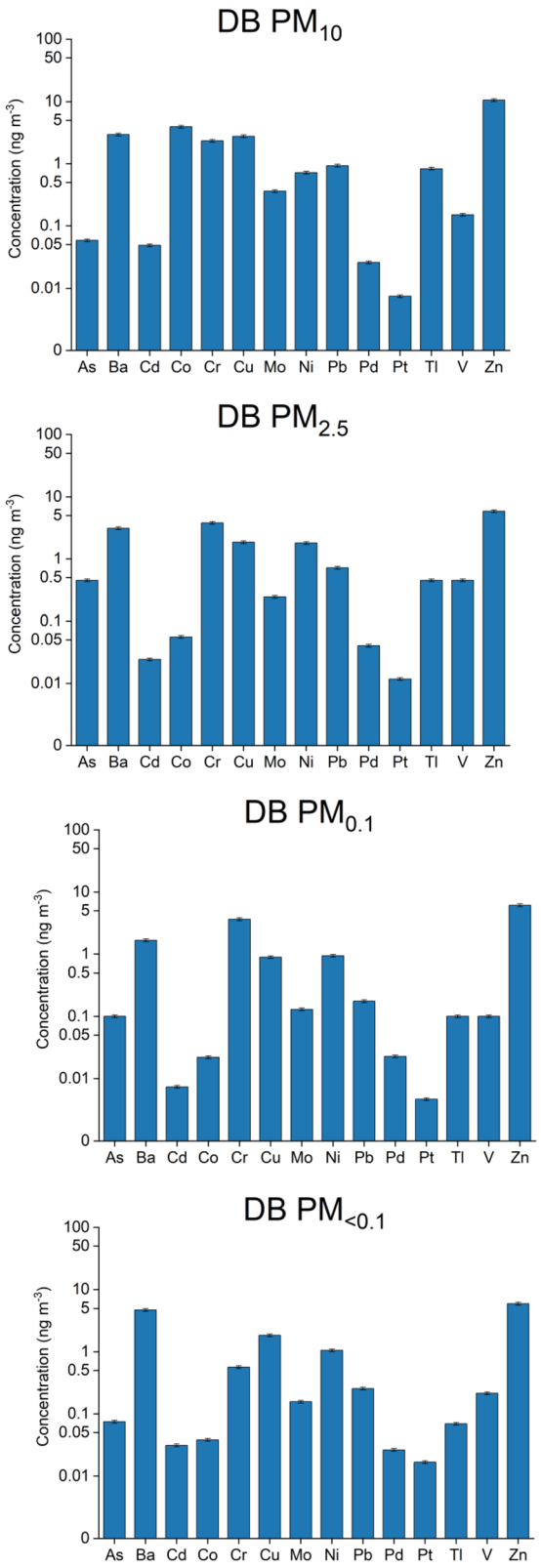

Fig. 3 *(contd,)*

2023 at three different urban settings in Slovenia: Dobrova (DB), Ljubljana (LJ) and Maribor (MB). LJ, the Slovenian capital, and MB, the second-largest city, represent densely populated areas with significant traffic-related emissions. In contrast, DB is a residential area located approximately 10 km from LJ, characterised by more localised sources of air pollution. PM samples were collected within one metre of bicycle lanes. Concentrations of metal(oid)s, PGEs and PAHs in the size-fractionated PM were determined using optimised analytical procedures. The results for metal(oid)s and PGEs are presented in Fig. 3, while the results for PAHs are shown in Fig. 4.

Fig. 3 (continued) shows the distribution of metal(oid)s in size-fractionated airborne PM in Maribor (MB), Ljubljana (LJ) and Dobrova (DB).

As shown in Fig. 3, the highest concentrations of metal(oid)s are primarily found in PM_{10} particles, with lower concentrations observed in $PM_{2.5}$ and $PM_{0.1}$. In the $PM_{<0.1}$ fraction, the concentrations of metal(oid)s (Ba, Cd, Cu, Ni, Pb, Pd, Pt, V and Zn) originating from traffic-related and coal combustion as well biomass sources, increased again to levels similar to those observed in PM_{10}. This indicates that the $PM_{<0.1}$ fraction, which penetrates most deeply into lung tissue and is potentially the most harmful to health, contributes significantly to the overall exposure to metal(oid)s.

The origin of As, Cr, Ni, Pb and V is primarily linked to high-temperature processes and fossil fuel combustion.[37,40,69,70] Ba, Cr, Cu, Mo, Pb, V and Zn are associated with gasoline engines,[38,49] while Ba, Cu and Mo arre related to lubricants and additives used in brake pads. Ba, Cd and Zn are linked to tyre wear[38] and Pd and Pt originate from catalyst emissions in car exhausts.[51]

The data in Fig. 3 further show that the highest concentrations of metal(oid)s were recorded at MB and LJ, as these sites are impacted by relatively dense traffic and are moderately populated, with populations of approximately 100 000 and 350 000, respectively. Lower metal(oid) concentrations were found at DB, which is a less densely populated residential area with less traffic. Additionally, LJ and MB also have a stronger presence of industrial facilities, including energy production plants, chemical manufacturing sites, and metal processing and waste management facilities.

Among metal(oid)s, Ba, Cr, Cu, Ni and Zn were measured in the highest concentrations in all size-fractioned PM, being elements typically associated with vehicular emissions. In MB, the PM_{10} fraction exhibited higher concentrations of As, Ba, Cr, Cu, Ni, Pb, and Zn compared to other fractions and locations, suggesting a more pronounced resuspension process and dust redistribution from both natural and anthropogenic sources.

In the PM_{10} fraction, Zn concentrations reached approximately 70 ng m^{-3} in MB and up to 15 ng m^{-3} in LJ, while Ba concentrations were around 30 ng m^{-3} in MB and 7 ng m^{-3} in LJ. Concentrations were significantly lower than those reported in larger cities, such as Fez in Morocco (with a population of about 1.1 million) or Changsha, China, where concentrations reached up to 250 ng m^{-3} for Zn and 70 ng m^{-3} for Ba.[66,67] The concentrations of Zn and Ba determined in DB in the PM_{10} fraction (Fig. 3) reached up to 10 ng m^{-3} for Zn and 5 ng m^{-3} for Ba, showing slightly lower concentrations than those reported by Jandacka *et al.*[41] for PM_{10} in the smaller city of Žilina, Slovakia (approximately 80 000 inhabitants). Across all observed

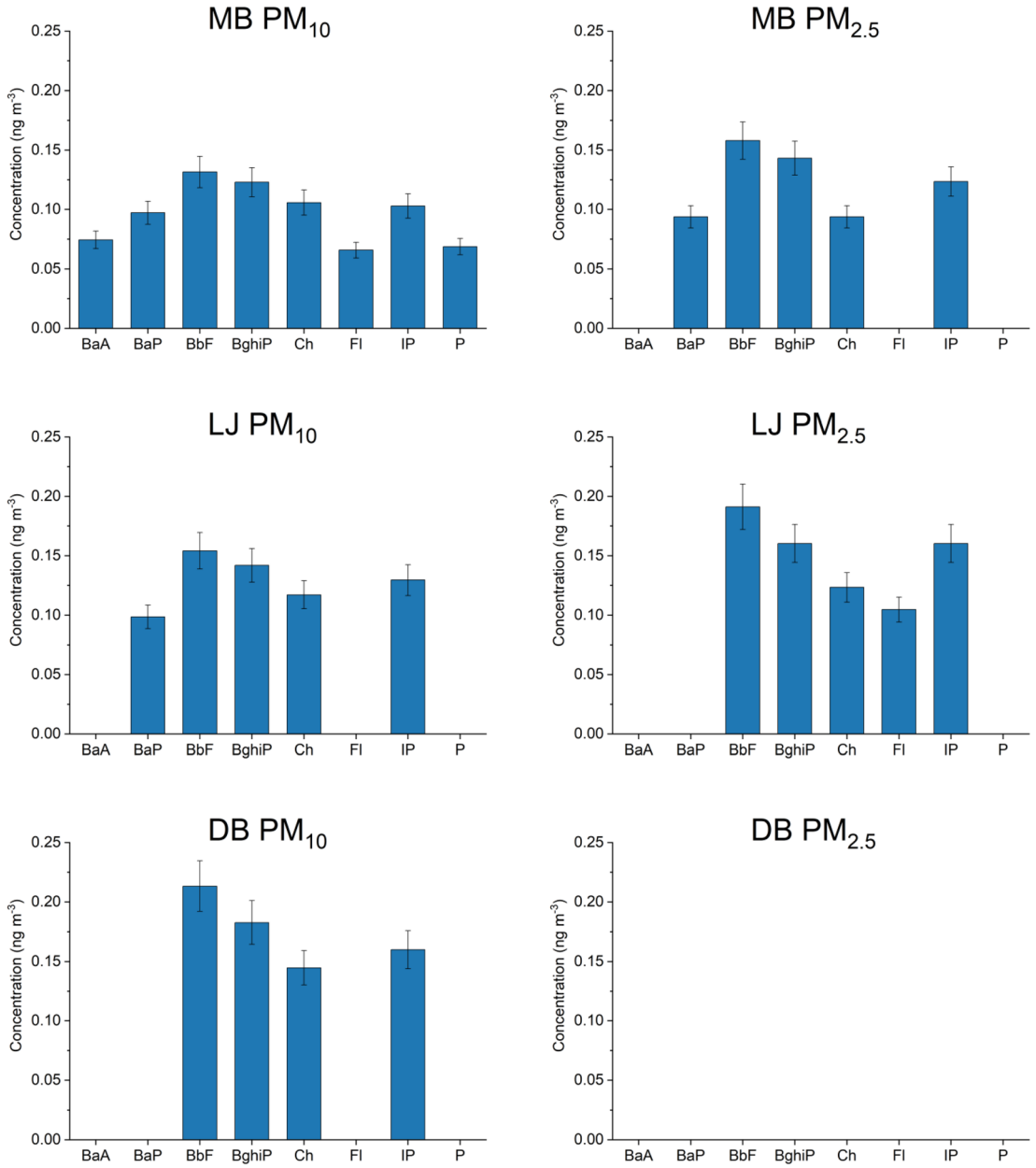

Fig. 4 The distribution of PAHs in size-fractionated airborne PM in Maribor (MB), Ljubljana (LJ) and Dobrova (DB).

PM fractions from this study (2.8–61.5 ng m^{-3} for Zn; 0.45–28.0 ng m^{-3} for Ba), concentrations were similar to those in Turin, Italy, where Zn varied between 5 and 90 ng m^{-3} for 0.54–11 μm PM fractions,[44] and to those reported in the Los Angeles area,[38] where Zn varied between 6 ng m^{-3} and 8.7 ng m^{-3} for PM_{10} and $PM_{2.5}$ respectively, and Ba between 16.5 ng m^{-3} and 14.9 ng m^{-3}. Ba and Zn, most abundant in coarse PM fractions, are typical of tyre and brake wear. Since their emissions are largely unaffected by fuel type or emission standards, this contributes to the observed similarities in their concentrations across different cities.

The highest concentrations of Cu in MB in the PM_{10} fraction (around 30 ng m^{-3}) were similar to those reported in Fez, Morocco,[67] while Ni concentrations in MB (around 2.5 ng m^{-3}) were significantly lower than those reported in Fez (95 ng m^{-3}). At the DB and LJ sampling sites, Cu concentrations in the PM_{10} fraction ranged from 2.8 and 12 ng m^{-3}, which is lower than the levels reported for Žilina (20 ng m^{-3}).[41] Ni concentrations in the PM_{10} fraction ranging from 0.7 to 2.7 ng m^{-3} were similar to those reported for Žilina (0.6 ng m^{-3}).[41] Additionally, Cu (0.15–28.6 ng m^{-3}) and Ni (0.28–2.7 ng m^{-3}) values across all PM fractions were similar to those reported in Leipzig (0.14–50 ng m^{-3} for Cu; 0.02–2.3 ng m^{-3} for Ni)[36] and Los Angeles (7.5 ng m^{-3} for Cu; 0.4–0.5 ng m^{-3} for Ni).[38] In Changsha, China,[66] Cu values across PM > 9 μm and PM < 0.4 μm varied between 10 and 20 ng m^{-3}. In Turin, Italy, Cu and Ni across 0.54–11.0 μm PM fractions varied from 0.5–3.3 ng m^{-3} and 0.5–6.0 ng m^{-3}, respectively.[44] Similarly to Ba and Zn, Cu concentrations are

mainly influenced by non-exhaust traffic emissions, resulting in similar Cu emission profiles. In contrast, Ni is more characteristic of gasoline and diesel vehicles.

The levels of Pb in MB in PM_{10} (4 ng m^{-3}) and $PM_{2.5}$ as well as $PM_{<0.1}$ (0.4 ng m^{-3}) were similar to those observed across all PM fractions in Turin, Italy (0.25–4.5 ng m^{-3}).[44] In Los Angeles,[38] average Pb concentrations in $PM_{2.5}$ and PM_{10} varied between 0.7 and 1.9 ng m^{-3}, significantly lower than those found in Fez (around 40 ng m^{-3})[67] and Changsha, China (30−120 ng m^{-3}),[66] but higher than Pb concentrations at other sampling sites in this study (0.9 to 2.6 ng m^{-3}) and in those reported for Žilina (1.7 ng m^{-3}).[41] The concentrations of Cr in the PM_{10} fraction were also the highest in MB (around 10 ng m^{-3}) and in LJ in PM_{10} and $PM_{0.1}$ (around 4 ng m^{-3}). In $PM_{<0.1}$, Cr varied between 0.12 and 0.88 ng m^{-3}. Concentrations were lower than those reported for Fez (35 ng m^{-3})[67] and Changsha (15−20 ng m^{-3}).[66] However, they were similar to those measured in Turin (0.3–2.5 ng m^{-3}) and Los Angeles (0.8–1.4 ng m^{-3}).[38,44] At other sampling sites in this study, Cr in the PM_{10} fraction was considerably lower (between 2.3 and 4 ng m^{-3}) and similar to the concentration level of Cr in Žilina (1.7 ng m^{-3}).[41] Higher concentrations of Pb in MB can be attributed to industrial activities such as metal processing and battery manufacturing, along with exhaust emissions. Similarly elevated concentrations of Cd, Cu and Zn were also attributed to the anthropogenic activities in the local area.[67]

In the PM_{10} fraction, As concentrations in MB were 1.2 ng m^{-3}, while at other sampling sites, the levels reached 0.5 ng m^{-3}, which is similar to the reported As concentration in Žilina.[41] As in $PM_{0.1}$ and $PM_{<0.1}$ across all observed locations varied between 0.02 and 0.11 ng m^{-3}. As in Turin, Italy[44] in the PM fraction 0.54–11 μm varied between 0.04 and 0.16 ng m^{-3}. Cd concentrations at all sampling sites were very low, ranging from 0.05 to 0.2 ng m^{-3}. In Los Angeles,[38] Cd concentrations in $PM_{2.5}$ and PM_{10} varied between 0.013 and 0.047 ng m^{-3}. Co, Mo, V and Tl were also found at low levels, with concentrations not exceeding 2 ng m^{-3}.

As expected, PGEs (Pd and Pt) related to the traffic emissions were present in low concentrations at all sampling sites. Across all size fractions, Pd concentrations were generally higher than those of Pt. Pt concentrations varied between 0.002 and 0.02 ng m^{-3}, while Pd ranged from 0.01 to 0.09 ng m^{-3}. These concentrations are similar to those reported for side streets, non-urban and rural areas with low traffic near Frankfurt, Germany,[43,69] and in aerosols from cities around the world, except for metropolitan areas such as Beijing, where Pt and Pd concentrations were significantly higher (around 0.2 and 0.8 ng m^{-3}, respectively).[51] In Changsha, China,[66] Pd concentrations in PM_{10} and $PM_{2.5}$ averaged around 0.02 ng m^{-3}.

Despite the differences in city size between the urban areas selected in this study and larger cities like Turin or Los Angeles, the similar chemical fingerprinting of size-fractionated PM (PM_{10} and $PM_{2.5}$) suggests comparable pollution level profiles for selected metal(oid)s. This may be attributed to more localised emission sources in Slovenian cities, higher traffic density per unit volume of air, and limited dispersion of air pollutants. Additionally, the timing and location of sampling also plays a significant role in comparability of detected metal(oid)s; for instance, PM sampling in Turin and Fez was conducted on rooftops, reflecting a greater influence of meteorological and regional emission factors rather than direct local exposure to traffic-related emissions.

High-molecular-weight PAHs (BaA, BaP, BbF, BghiP, Ch, Fl, IP and P), typically bound to particles, were found in the highest concentrations in the PM_{10} fraction. They were also present in the $PM_{2.5}$ fraction at the MB and LJ sampling sites, but were not detected in the $PM_{0.1}$ and $PM_{<0.1}$ fractions. BbF, BghiP and IP, 5- and 6-ring PAHs typically associated with traffic-related sources exhibited higher concentrations in the $PM_{2.5}$ fraction. Their concentrations were low, ranging from 0.07 to 0.2 ng m^{-3}. BbF, BghiP and IP values in PM_{10}, $PM_{2.5}$ and PM_1 observed in Zagreb, Croatia (population about one million)[71] were higher, ranging between 0.4 and 3.4 ng m^{-3}. Higher PAH concentrations (with the sum of PAHs in the PM_{10} fraction ranging from 7 to 10 ng m^{-3}) were reported for the large city of Fez.[68] Comparable concentrations of PAHs to those reported in our study were found by Xing *et al.*[72] in Kanazawa, Japan (population of about 450 000). They observed that the sum of 9 PAHs (Fl, P, BaA, Ch, BbF, BkF, BaP BghiP and IP) in the $PM_{2.5}$ fraction ranged from 0.2 ng m^{-3} in summer to 1 ng m^{-3} in winter. A similarly low sum of PAHs (1–2.1 ng m^{-3}) was reported by Jedynska *et al.*[73] in PM_{10} and $PM_{2.5}$ fractions observed in Rome, Copenhagen, London and Oslo. For comparison, in our study conducted in MB in December 2024, the sum of 8 PAHs in PM_{10} was 0.8 ng m^{-3} and in $PM_{2.5}$ was 0.7 ng m^{-3}. In LJ, the sum of 8 PAHs in the PM_{10} fraction was 0.7 ng m^{-3}, while in the $PM_{2.5}$ fraction, it was 0.8 ng m^{-3}. The presence of high-molecular-weight PAHs can be attributed to traffic emissions as well as biomass burning.[33–35]

BaP, characterised as one of the most carcinogenic PAHs, varied between <0.02 ng m^{-3} and 0.1 ng m^{-3}, with the highest concentrations observed in the PM_{10} fraction in MB. The data from the literature show that the concentration of BaP in Porto varied between 0.01 ng m^{-3} and 2.7 ng m^{-3}, with an average value of 0.37 ng m^{-3}; while in Athens it averaged at 0.25 ng m^{-3} and 0.21 ng m^{-3} in Copenhagen.[73] In Zagreb, Croatia,[71] BaP in PM_{10}, $PM_{2.5}$ and PM_1 varied between 0.8 ng m^{-3} and 2 ng m^{-3}.

Certain compounds, such as As, Cd, Ni and BaP, are identified as human genotoxic carcinogens. The European Union Directive (Directive 2004/107/EC 2004)[74] has established threshold levels to mitigate their harmful effects on human health, with annual target values set for PM_{10} at 6 ng m^{-3} for As, 5 ng m^{-3} for Cd, 20 ng m^{-3} for Ni and 1 ng m^{-3} for BaP. In this study, none of the target values were exceeded in any size-fractioned PM samples. Threshold limits for other metal(oid)s, PGEs and PAHs for finer PM fractions have not yet been established.

The results of this study revealed that metal(oid)s, PGEs and PAHs are primarily attributed to anthropogenic activities, particularly traffic emissions and biomass burning. However, their concentrations at the selected sampling sites, located within one metre of bicycle lanes, were low, indicating that the pollution-related health risks for daily commuters are minimal.

The developed sampling device for size-fractionated PM, in combination with optimised analytical procedures, enables reliable and sensitive analysis of metal(loid)s, PGEs and PAHs at very low concentrations and is also applicable in areas with high levels of air pollution. It makes a significant contribution to improving air pollution control and legislation, identifying the sources of air pollution and assessing the associated health and environmental risks.

Conclusions

In this study, a sampling device was developed, consisting of low-volume cascade PTFE membrane filter system (PM_{10}, $PM_{2.5}$, and $PM_{0.1}$), connected to an ultrapure water trap that retains the nano-sized fraction ($PM_{<0.1}$). When combined with optimised analytical procedures, this setup provides a reliable analytical tool for detecting metal(oid)s, PGEs and PAHs, including those bound to nano-sized fractions, a capability not achievable with previous sampling devices that relied solely on filters for PM fractionation, thus enabling a more accurate residential exposure assessment.

The applicability of the sampling device was demonstrated through a one-month study conducted at three different locations in Slovenia, which differ in size, population and traffic density. The results revealed that the highest concentrations of metal(oid)s and PGEs were predominantly found in the PM_{10} fraction, largely influenced by resuspension processes and dust redistribution. Trace elements linked to traffic related emissions, both exhaust and non-exhaust, as well as coal and biomass combustion (Ba, Cd, Cu, Ni, Pb, Pd, Pt, V, and Zn) were significantly elevated in $PM_{<0.1}$ across all sampling locations, indicating the importance of characterising this size range. High-molecular-weight PAHs were distributed between PM_{10} and $PM_{2.5}$ fractions, with 5-ring (BaP and BbF) and 6-ring (BghiP and IP) PAH compounds, typically associated with traffic emissions, found in higher concentrations in the $PM_{2.5}$ fraction. Contaminant concentrations were low, indicating the minimal pollution-related health risks for daily commuters using bicycle lanes.

This one-month study, incorporating a newly developed sampling device, will be further expanded into a systematic one-year study to analyse size-fractionated PM samples across urban areas in Slovenia.

Author contributions

AI: writing – original draft, methodology, analysis, data curation, conceptualisation. RMŠ: writing – review & editing, supervision, methodology, conceptualisation. MĐ: analysis, writing – review & editing. AMP: resources, project administration, funding acquisition, review & editing. JŠ: funding acquisition, writing – review & editing, supervision, methodology.

Conflicts of interest

There are no conflicts to declare.

Data availability

The data supporting this article have been included as part of the SI. See DOI: https://doi.org/10.1039/d5ay00858a.

Acknowledgements

The authors acknowledge Mateja Štefančič (PhD) and Mateja Košir (PhD) for morphological analysis. The authors acknowledge financial support from the Slovenian Research and Innovation Agency (ARIS), specifically from the Developmental Funding Pillar (SI: "razvojni steber financiranja, RSF"), and ARIS financial support in programme groups P2-0273 and P1-0143.

References

1 M. J. Gatari, J. Boman, A. Wagner, S. Janhäll and J. Isakson, Assessment of inorganic content of PM2.5 particles sampled in a rural area north-east of Hanoi, Vietnam, *Sci. Total Environ.*, 2006, **368**(2), 675–685.
2 J. Kukutschová, P. Moravec, V. Tomášek, V. Matějka, J. Smolík, J. Schwarz, *et al.* On airborne nano/micro-sized wear particles released from low-metallic automotive brakes, *Environ. Pollut.*, 2011, **159**(4), 998–1006.
3 P. Pant and R. M. Harrison, Estimation of the contribution of road traffic emissions to particulate matter concentrations from field measurements: A review, *Atmos. Environ.*, 2013, **77**, 78–97.
4 P. Sanderson, J. M. Delgado-Saborit and R. M. Harrison, A review of chemical and physical characterisation of atmospheric metallic nanoparticles, *Atmos. Environ.*, 2014, **94**, 353–365.
5 A. Thorpe and R. M. Harrison, Sources and properties of non-exhaust particulate matter from road traffic: A review, *Sci. Total Environ.*, 2008, **400**(1), 270–282.
6 W. Lin, H. Zhang, Y. Lai, S. Zhuang, Q. Wei, S. Fu, *et al.* Source-Specific Ecological Risk of Atmospheric PM2.5-Bound Metals and Implications for Air Pollution Control: A Regional Perspective from China, *Expo Health*, 2024, **16**(3), 745–757.
7 W. H. Shetaya, A. El-Mekawy and S. K. Hassan, Tempo-Spatial Variability and Health Risks of PM2.5 and Associated Metal(loid)s in Greater Cairo, Egypt, *Expo Health*, 2024, **16**(4), 973–988.
8 Y. Wu, N. Zhang, Y. Shi, Z. Chen, H. Zhang, J. Yin, *et al.* PAH Pollution and Risk in Particulate Matter in Chinese Cities, *Exposure Health*, 2024, **16**, 401–415.
9 H. Chen, M. S. Goldberg and P. J. Villeneuve, A systematic review of the relation between long-term exposure to ambient air pollution and chronic diseases, *Rev. Environ. Health*, 2008, **23**(4), 243–297.
10 A. J. Cohen, M. Brauer, R. Burnett, H. R. Anderson, J. Frostad, K. Estep, *et al.* Estimates and 25-year trends of the global burden of disease attributable to ambient air pollution: an analysis of data from the Global Burden of Diseases Study, *Lancet*, 2015, **389**(10082), 1907–1918.

11 F. J. Kelly and J. C. Fussell, Size, source and chemical composition as determinants of toxicity attributable to ambient particulate matter, *Atmos. Environ.*, 2012, **60**, 504–526.
12 H. Kim, W. H. Kim, Y. Y. Kim and H. Y. Park, Air Pollution and Central Nervous System Disease: A Review of the Impact of Fine Particulate Matter on Neurological Disorders, *Public Health Front.*, 2020, **8**, 575330.
13 A. G. Russell and B. Brunekreef, A Focus on Particulate Matter and Health, *Environ. Sci. Technol.*, 2009, **43**(13), 4620–4625.
14 Y. Wang, L. Xiong and M. Tang, Toxicity of inhaled particulate matter on the central nervous system: neuroinflammation, neuropsychological effects and neurodegenerative disease, *J. Appl. Toxicol.*, 2017, **37**(6), 644–667.
15 A. Valavanidis, K. Fiotakis and T. Vlachogianni, Airborne Particulate Matter and Human Health: Toxicological Assessment and Importance of Size and Composition of Particles for Oxidative Damage and Carcinogenic Mechanisms, *J. Environ. Sci. Health, Part C*, 2008, **26**(4), 339–362.
16 US EPA, 2019, *Integrated Science Assessment (ISA) for Particulate Matter (Final Report, Dec 2019)*.
17 M. Lippmann, *The US EPA Standards for Particulate Matter and Ozone*, Royal Society of Chemistry, 1997, pp. 75–99.
18 W. MacNee and K. Donaldson, Mechanism of lung injury caused by PM10 and ultrafine particles with special reference to COPD, *Eur. Respir. J.*, 2003, 47–51.
19 I. Drventić, M. Šala, K. Vidović and A. Kroflič, Direct quantification of PAHs and nitro-PAHs in atmospheric PM by thermal desorption gas chromatography with electron ionization mass spectroscopic detection, *Talanta*, 2023, **251**, 123761.
20 J. Sánchez-Piñero, J. Moreda-Piñeiro, E. Concha-Graña, M. Fernández-Amado, S. Muniategui-Lorenzo and P. López-Mahía, Inhalation bioaccessibility estimation of polycyclic aromatic hydrocarbons from atmospheric particulate matter (PM10): Influence of PM10 composition and health risk assessment, *Chemosphere*, 2021, **263**, 127847.
21 D. Saraga, T. Maggos, C. Degrendele, J. Klánová, M. Horvat, D. Kocman, *et al.* Multi-city comparative PM2.5 source apportionment for fifteen sites in Europe: The ICARUS project, *Sci. Total Environ.*, 2021, **751**, 141855.
22 J. Szabó, A. Nagy and J. Erdős, Ambient concentrations of PM10, PM10-bound polycyclic aromatic hydrocarbons and heavy metals in an urban site of Győr, Hungary, *Air Qual., Atmos. Health*, 2015, **8**, 229–241.
23 S. Karthikeyan, U. M. Joshi and R. Balasubramanian, Microwave assisted sample preparation for determining water-soluble fraction of trace elements in urban airborne particulate matter: evaluation of bioavailability, *Anal. Chim. Acta*, 2006, **576**(1), 23–30.
24 C. Marina-Montes, E. Abás, J. Buil-García and J. Anzano, From multi to single-particle analysis: A seasonal spectroscopic study of airborne particulate matter in Zaragoza, Spain, *Talanta*, 2023, **259**, 124550.
25 R. Milačič, H. Leskovšek, F. Dolinšek and D. Hrček, A complex study of air pollution with cadmium, lead, polycyclic aromatic hydrocarbons, sulfur dioxide, and black smoke in the Zasavje industrialized urban region in Slovenia, *Ann. Chim*, 1995, **85**, 131–148.
26 D. Salcedo, J. P. Bernal, O. Pérez-Arvizu and E. Lounejeva, Assessment of sample preparation methods for the analysis of trace elements in airborne particulate matter, *J. Anal. At. Spectrom.*, 2014, **29**(4), 753–761.
27 L. Samek, Z. Stegowski, K. Styszko, L. Furman and J. Fiedor, Seasonal contribution of assessed sources to submicron and fine particulate matter in a Central European urban area, *Environ. Pollut.*, 2018, **241**, 406–411.
28 N. Zioła and K. Słaby, The Content of Selected Heavy Metals and Polycyclic Aromatic Hydrocarbons (PAHs) in PM10 in Urban-Industrial Area, *Sustainability*, 2020, **13**, 5284.
29 L. H. Keith, The Source of U.S. EPA's Sixteen PAH Priority Pollutants, *Polycyclic Aromat. Compd.*, 2015, **35**(2–4), 147–160.
30 US EPA, 2017, *Polycyclic Aromatic Hydrocarbons (PAHs) - Integrated Risk Information System (IRIS)*.
31 WHO, Some Non-heterocyclic Polycyclic Aromatic Hydrocarbons and Some Related Exposures, *Int. Agency Res. Cancer*, 2010, **92**, 819.
32 International Agency for Research on Cancer. 2016, *Outdoor Air Pollution 109*.
33 W. Insian, N. Yabueng, W. Wiriya and S. Chantara, Size-fractionated PM-bound PAHs in urban and rural atmospheres of northern Thailand for respiratory health risk assessment, *Environ. Pollut.*, 2022, **293**, 118488.
34 R. Shen, Y. Wang, W. Gao, X. Cong, L. Cheng and X. Li, Size-segregated particulate matter bound polycyclic aromatic hydrocarbons (PAHs) over China: Size distribution, characteristics and health risk assessment, *Sci. Total Environ.*, 2019, **685**, 116–123.
35 Q. Yu, X. Ding, Q. He, W. Yang, M. Zhu, S. Li, *et al.* Nationwide increase of polycyclic aromatic hydrocarbons in ultrafine particles during winter over China revealed by size-segregated measurements, *Atmos. Chem. Phys.*, 2020, **20**(23), 14581–14595.
36 K. W. Fomba, D. van Pinxteren, K. Müller, G. Spindler and H. Herrmann, Assessment of trace metal levels in size-resolved particulate matter in the area of Leipzig, *Atmos. Environ.*, 2018, **176**, 60–70.
37 Y. Gao and H. Ji, Microscopic morphology and seasonal variation of health effect arising from heavy metals in PM2.5 and PM10: One-year measurement in a densely populated area of urban Beijing, *Atmos. Res.*, 2018, **212**, 213–226.
38 F. Oroumiyeh, M. Jerrett, I. Del Rosario, J. Lipsitt, J. Liu, S. E. Paulson, *et al.* Elemental composition of fine and coarse particles across the greater Los Angeles area: Spatial variation and contributing sources, *Environ. Pollut.*, 2022, **292**, 118356.
39 V. Evagelopoulos, N. D. Charisiou and S. Zoras, Dataset of Polycyclic aromatic hydrocarbons and trace elements in

PM2.5 and PM10 atmospheric particles from two locations in North-Western Greece, *Data Brief*, 2022, **42**, 108266.

40 Y. Tian, B. Jia, P. Zhao, D. Song, F. Huang and Y. Feng, Size distribution, meteorological influence and uncertainty for source-specific risks: PM2.5 and PM10-bound PAHs and heavy metals in a Chinese megacity during 2011–2021, *Environ. Pollut.*, 2022, **312**, 120004.

41 D. Jandacka, D. Durcanska and M. Bujdos, The contribution of road traffic to particulate matter and metals in air pollution in the vicinity of an urban road, *Transp. Res. D: Transp. Environ.*, 2017, **50**, 397–408.

42 A. Teffahi, Y. Kerchich, Y. Moussaoui, P. Romagnoli, C. Balducci, C. Malherbe, *et al.* Exposure levels and health risk of PAHs associated with fine and ultrafine aerosols in an urban site in northern Algeria, *Air Qual., Atmos. Health*, 2021, **14**(9), 1375–1391.

43 F. Zereini, H. Alsenz, C. L. S. Wiseman, W. Püttmann, E. Reimer, R. Schleyer, *et al.* Platinum group elements (Pt, Pd, Rh) in airborne particulate matter in rural *vs.* urban areas of Germany: Concentrations and spatial patterns of distribution, *Sci. Total Environ.*, 2012, **416**, 261–268.

44 M. Malandrino, M. Casazza, O. Abollino, C. Minero and V. Maurino, Size resolved metal distribution in the PM matter of the city of Turin (Italy), *Chemosphere*, 2016, **147**, 477–489.

45 V. Celo, E. Dabek, D. Mathieu and I. Okonskaia, Validation of a Simple Microwave-Assisted Acid Digestion Method Using Microvessels for Analysis of Trace Elements in Atmospheric PM2.5 in Monitoring and Fingerprinting Studies, *Open Chem. Biomed. Methods J.*, 2010, **3**, 141–150.

46 E. Dabek-Zlotorzynska, Validation of a Simple Microwave-Assisted Acid Digestion Method Using Microvessels for Analysis of Trace Elements in Atmospheric PM2.5 in Monitoring and Fingerprinting Studies, *Open Chem. Biomed. Methods J.*, 2010, **3**(1), 143–152.

47 P. K. Hopke, Q. Dai, L. Li and Y. Feng, Global review of recent source apportionments for airborne particulate matter, *Sci. Total Environ.*, 2020, **740**, 140091.

48 S. A. Wise and R. L. Watters, 2020, *Standard Reference Material 1648a - Urban Particulate Matter, Certificate Analysis*, Gaithersburg.

49 P. Coufalík, P. Mikuška, T. Matoušek and Z. Večeřa, Determination of the bioaccessible fraction of metals in urban aerosol using simulated lung fluids, *Atmos. Environ.*, 2016, **140**, 469–475.

50 R. Viskup, Comparison of Different Techniques for Measurement of Soot and Particulate Matter Emissions from Diesel Engine Introduction to Diesel Emissions, *IntechOpen*, 2020, 1–19.

51 L. Zhang, Y. Wang, Y. Liu, Z. Li and X. Li, Variation of platinum group elements (PGE) in airborne particulate matter (PM2.5) in the Beijing urban area, China: A case study of the 2014 APEC summit, *Atmos. Environ.*, 2019, **198**, 70–76.

52 SIST ISO 18287:2019, *Soil Quality - Determination of Polycyclic Aromatic Hydrocarbons (PAH) - Gas Chromatographic Method with Mass Spectrometric Detection (GC-MS)*, 2019.

53 SIST EN 15527:2009, *Characterization of Waste - Determination of Polycyclic Aromatic Hydrocarbons (PAH) in Waste Using Gas Chromatography Mass Spectrometry (GC/MS)*, 2009.

54 EN 15549:2008, *Air Quality - Standard Method for the Measurement of the Concentration of Benzo[a]pyrene in Ambient Air*, 2008.

55 ISO 28540:2011, *Water Quality — Determination of 16 Polycyclic Aromatic Hydrocarbons (PAH) in Water — Method Using Gas Chromatography with Mass Spectrometric Detection (GC-MS)*, 2011.

56 K. Ravindra, R. Sokhi and R. Van Grieken, Atmospheric polycyclic aromatic hydrocarbons: Source attribution, emission factors and regulation, *Atmos. Environ.*, 2008, **42**(13), 2895–2921.

57 R. Roy, R. Jan, G. Gunjal, R. Bhor, K. Pai and P. G. Satsangi, Particulate matter bound polycyclic aromatic hydrocarbons: Toxicity and health risk assessment of exposed inhabitants, *Atmos. Environ.*, 2019, **210**, 47–57.

58 F. Usman, B. Zeb, K. Alam, Z. Huang, A. Shah, I. Ahmad, *et al.* In-Depth Analysis of Physicochemical Properties of Particulate Matter (PM10, PM2.5 and PM1) and Its Characterization through FTIR, XRD and SEM–EDX Techniques in the Foothills of the Hindu Kush Region of Northern Pakistan, *Atmosphere*, 2022, **13**(1), 124.

59 B. Zeb, K. Alam, A. Sorooshian, T. Blaschke, I. Ahmad and I. Shahid, On the Morphology and Composition of Particulate Matter in an Urban Environment, *Aerosol Air Qual. Res.*, 2018, **18**(6), 1431–1447.

60 S. Romano, Bioaerosols: Composition, Meteorological Impact, and Transport, *Atmosphere*, 2023, **14**(3), 590.

61 G. Carabali, R. Mamani-Paco, T. Castro, O. Peralta, E. Herrera and B. Trujillo, Optical properties, morphology and elemental composition of atmospheric particles at T1 supersite on MILAGRO campaign, *Atmos. Chem. Phys.*, 2012, **12**(5), 2747–2755.

62 C. A. Breed, J. M. Arocena and D. Sutherland, Possible sources of PM10 in Prince George (Canada) as revealed by morphology and *in situ* chemical composition of particulate, *Atmos. Environ.*, 2002, **36**(10), 1721–1731.

63 L. T. González, F. E. Longoria-Rodríguez, M. Sánchez-Domínguez, C. Leyva-Porras, K. Acuña-Askar, B. I. Kharissov, *et al.* Seasonal variation and chemical composition of particulate matter: A study by XPS, ICP-AES and sequential microanalysis using Raman with SEM/EDS, *J. Environ. Sci.*, 2018, **74**, 32–49.

64 W. Li and L. Shao, Transmission electron microscopy study of aerosol particles from the brown hazes in northern China, *J. Geophys. Res.:Atmos.*, 2009, **114**, D09302.

65 Z. Wang, L. Zhang, Y. Zhang, Z. Zhao and S. Zhang, Morphology of single inhalable particle in the air polluted city of Shijiazhuang, China, *J. Environ. Sci.*, 2008, **20**(4), 429–435.

66 X. Liu, Y. Zhai, Y. Zhu, Y. Liu, H. Chen, P. Li, *et al.* Mass concentration and health risk assessment of heavy metals in size-segregated airborne particulate matter in Changsha, *Sci. Total Environ.*, 2015, **517**, 215–221.

67 M. Gaberšek, M. J. Watts and M. Gosar, Attic dust: an archive of historical air contamination of the urban environment and potential hazard to health?, *J. Hazard. Mater.*, 2022, **432**, 128745.

68 N. Deabji, K. W. Fomba, E. J. dos Santos Souza, A. Mellouki and H. Herrmann, Influence of anthropogenic activities on metals, sugars and PAHs in PM10 in the city of Fez, Morocco: Implications on air quality, *Environ. Sci. Pollut. Res.*, 2024, **31**(17), 25238–25257.

69 F. Zereini, F. Alt, J. Messerschmidt, A. von Bohlen, K. Liebl and W. Püttmann, Concentration and distribution of platinum group elements (Pt, Pd, Rh) in airborne particulate matter in Frankfurt am Main, Germany, *Environ. Sci. Technol.*, 2004, **15–38**(6), 1686–1692.

70 E. Sarti, L. Pasti, M. Rossi, M. Ascanelli, A. Pagnoni, M. Trombini, *et al.* The composition of PM1 and PM2.5 samples, metals and their water soluble fractions in the Bologna area (Italy), *Atmos. Pollut. Res.*, 2015, **6**(4), 708–718.

71 I. Jakovljević, G. Pehnec, V. Vađić, M. Čačković, V. Tomašić and J. D. Jelinić, Polycyclic aromatic hydrocarbons in PM10, PM2.5 and PM1 particle fractions in an urban area, *Air Qual., Atmos. Health*, 2018, **11**(7), 843–854.

72 W. Xing, L. Zhang, L. Yang, Q. Zhou, X. Zhang, A. Toriba, *et al.* Characteristics of PM2.5-Bound Polycyclic Aromatic Hydrocarbons and Nitro-Polycyclic Aromatic Hydrocarbons at A Roadside Air Pollution Monitoring Station in Kanazawa, Japan, *Int. J. Environ. Res. Public Health*, 2020, **17**(3), 805.

73 A. Jedynska, G. Hoek, M. Eeftens, J. Cyrys, M. Keuken, C. Ampe, *et al.* Spatial variations of PAH, hopanes/steranes and EC/OC concentrations within and between European study areas, *Atmos. Environ.*, 2014, **87**, 239–248.

74 *Directive 2004/107/EC of the European Parliament and of the Council of 15 December 2004 Relating to Arsenic, Cadmium, Mercury, Nickel and Polycyclic Aromatic Hydrocarbons in Ambient Air*, **https://eur-lex.europa.eu/LexUriServ/LexUriServ.do?uri=OJ:L:2005:023:0003:0016:EN:PDF**.